Random lasing behaviour in Al-doped ZnO nanorods

Atiqah Nabieha Azmi[1], Wan Maryam Wan Ahmad Kamil[1*], Haslan Abu Hassan[1], Wan Zakiah Wan Ismail[2], Otto L. Muskens[3].

[1]School of Physics, Universiti Sains Malaysia, 11800 Gelugor, Penang, Malaysia.
[2]Faculty of Engineering and Built Environment, Universiti Sains Islam Malaysia, 71800 Nilai, Negeri Sembilan, Malaysia.
[3]Physics and Astronomy, Faculty of Physical Sciences and Engineering, University of Southampton, SO17 1BJ, United Kingdom.

*corresponding author: wanmaryam@usm.my

ABSTRACT

A novel method of doping Aluminum (Al) into zinc oxide (ZnO) nanorods by a simple chemical dip process is evaluated in terms of its performance in random lasing. The ZnO nanorods were synthesized by the chemical bath deposition (CBD) method at a fixed temperature of 96 °C for three hours. The ZnO nanorods were then dipped into a fixed doping solution concentration. The dip time was varied between 0 s to 80 s and a gradual increase of Al % from the nanorod array was observed with increasing dip time. Doping ZnO nanorods in aluminum nitrate nonahydrate solution for 40 s contributes to random lasing with the lowest threshold value of 12.48 mJ/cm^2 and a spectral width of 2.12 nm.

1. INTRODUCTION

The observation of random lasing is different from conventional lasers as it relies on nanostructures to trap photons through multiple photons scattering. It was first discovered in 1966 by replacing one of the laser mirrors in a Fabry-Perot cavity with a scattering medium [1]. Letokhov then modified the diffusion theory to introduce scattering by investigating the random walk of photons in a random system to theoretically prove random lasing emission [2]. A multimode laser spectrum without an external cavity was discovered in 1994 by Lawandy et al, showing the first working principle of a random laser [3].

Random lasers are used in numerous biosensor applications to detect cancerous thyroid, changes in structure and composition of brain tissues, small pH and temperature variations, uterine tissues, sense low levels of dopamine, and distinguish malignant and healthy tissues [4]-[10]. However, lowering of the lasing thresholds for advancing in this field is still a challenge. Numerous initiatives to lower the lasing thresholds include using dye-doped polymer films [11]–[13], altering the irradiated laser conditions [14], coupling the random cavity modes with planar microcavity modes [15], employing SnO_2 nanowires coated with an amorphous layer [16], doping of Al [17], doping of gold [18], and employing a SiO_2 capping layer with ZnO nanorods [19].

It has been demonstrated that doping ZnO with Al can reduce resistivity, increase transmittance in the visible area, obtain high conductivity, provide high sensitivity, generate extra electrons,

and increase the band gap energy [20]–[22]. Doping with Al was also reported to enhance photodetector performance due to long-term emission current stability, fast response and recovery time, and better electrical conductivity compared to pure ZnO [23]–[25]. These advantages make Al the ideal choice for doping with ZnO. In addition, Al is the most common doping element used in solution-based growth techniques to dope ZnO [26]–[28]. There are two methods to perform doping; in-situ and ex-situ. Our previous work on in-situ doping of Al revealed challenges in increasing the doping percentage whereby the maximum reported limit of doping concentrations was between 0.67 % [17] and 1.72 % [29]. In addition, a number of challenges that arise when employing the in-situ method of doping, include a significant distortion along the growth direction (c-axis) [30], decreased deposition rate [31] and slower growth rate [32].

To solve the problems associated with in-situ doping, we proposed simple ex-situ doping of ZnO nanostructure to increase the doping concentration in ZnO and hence further reduce the random lasing threshold. The ZnO nanostructure was synthesized by chemical bath deposition, and doping was done by dipping the ZnO structures into aluminum nitrate nonahydrate solution at different dipping durations then followed by annealing to enhance doping. The aluminum nitrate nonahydrate solution is a non-toxic, low-cost dopant solution, and low energy consumption was used to evaluate its efficiency in random lasing. The morphology, structural, optical and lasing properties were characterized, analyzed and discussed in this manuscript.

2. METHODOLOGY

2.1. Preparation of ZnO seed layer

Standard microscopic glass slides 1 mm thick and 7.5 cm x 2.5 cm in size was used as the substrate. The substrate was cleaned in a Branson 1510 ultrasonic bath with deionized water, acetone, and ethanol for 10 minutes each. Nitrogen gas was then used to dry the glass substrate. This cleaning procedure eliminates impurities from the glass surface to provide a very adhesive and high-quality surface for seed layer deposition. A 100 nm of ZnO seed layer was deposited using Auto HHV500 radio frequency sputtering with the base vacuum pressure of $5x10^{-5}$ mbar and operating power of 150 W. The deposited ZnO seed layer then undergoes heat treatment for 1 hour at 100 °C.

2.2 Preparation of ZnO nanorods

Chemicals were purchased from Sigma-Aldrich and used as received without any purification process. The ZnO nanorods were prepared using the chemical bath deposition (CBD) method. Both zinc nitrate ($Zn(NO_3)_2.6H_2O$), product number 228737 with a molar mass of 297.49 g/mol and hexamethylenetetramine (HMT) $(CH_2)_6N_4$, product number 33233 with a molar mass of 140.19 g/mol were used. The synthesis starts with diluting 50 ml of deionized water to form 0.08 M of zinc nitrate and 0.08 M of HMT, separately. Then, both solutions are combined and stirred for 1 minute. The ZnO seed layer-coated glass substrate was then placed vertically in the beaker containing a mixture of zinc nitrate and HMT. Note that, the glass substrate must be fully sinking in the solution to make sure the synthesis covers the entire glass substrate. The growth of ZnO nanorods was fixed at 96°C in a binder oven for 3 hours. The ZnO nanorods were then rinsed using deionised water to remove the excessive mass of ZnO. The chemical process during the CBD process is as follows:

$$(CH_2)_6N_4 + 6H_2O \rightarrow 6HCHO + 4NH_3$$

$$NH_3 + H_2O \leftrightarrow NH_4^+ + OH^-$$

$$Zn(NO_3)_2 \rightarrow Zn^{2+} + 2NO_3^-$$

$$Zn^{2+} + 2OH^- \leftrightarrow ZnO(s) + H_2O$$

2.3 Preparation of doping solution

Aluminum nitrate nonahydrate ($Al(NO_3)_3.9H_2O$) was diluted with 30 ml of deionized water and stirred for 10 minutes to form 10 mM of doping solution. The ZnO nanorods were then submerged in the doping solution for 0 s, 20 s, 30 s, 40 s, 60 s, and 80 s and samples were heated for one minute at 96 °C. Then, the samples were annealed in ambient air at 300°C for one hour. The reaction equation as ZnO nanorods dipped in aluminum nitrate nonahydrate solution is as follows [25]:

$$Al(NO_3)_2.9H_2O \rightarrow Al^{3+} + 3NO_3^- + 9H_2O$$

$$Al^{3+} + 3OH^- \rightarrow Al(OH)_3$$

$$Zn^{2+} + Al^{3+} + 5OH^- \rightarrow Zn(OH)_2 + Al(OH)_3$$

$$2Al(OH)_3 \leftrightarrow Al_2O_3 + 3H_2O$$

$$Zn(OH)_2 + 2Al(OH)_3 \leftrightarrow ZnO + Al_2O_3 + 4H_2O$$

2.4 Characterization method

Using a CuKα radiation source with wavelength of 1.5406 Å, PANalytical X'Pert PRO MRD PW3040 X-ray diffraction (XRD) analysis was used to evaluate the crystallinity of the samples. Meanwhile, the samples' morphology, distributions and atomic percentage of elements were determined using a field emission scanning electron microscope (FESEM) Nova NanoSEM 450 paired with energy-dispersive X-ray spectroscopy (EDX). Both room temperature photoluminescence (PL) and room temperature random laser measurements were performed using a 355 nm Nd:YAG laser source with 0.6 ns pulse width and 20 kHz repetition rate. The power of the laser source was varied from 31 mW to 0.91 mW. Ocean optics fibre spectrometer was used to record the emission, and Ocean View software was used to analyse the spectrum.

3. RESULTS AND DISCUSSION

Figure 1 shows the FESEM image of top and cross-sectional (inset) view for ZnO nanorods dipped in aluminum nitrate nonahydrate solution at various dipping times. Image J software was used to determine the average ZnO nanorod's diameter and height. Overall, the average ZnO nanorods diameter do not change significantly as the dipping time increases from 0 s to 80 s (± 14 nm). However, the height of ZnO nanorods shows an obvious reduction as the dipping duration increases from 1200 nm to 676 nm. Further investigation on the acidity of the aluminum nitrate nonahydrate solution reveals a pH of 4 (acidic solution). Previous reports mention ZnO nanorods will slowly dissolve at a pH ≤ 4.6 [33]. This is observed in our samples as shown in the cross-section FESEM image whereby increasing the dipping time reduces the

ZnO height. Important to note that during all dipping durations, the pH level of the aluminum nitrate nonahydrate solution was constant.

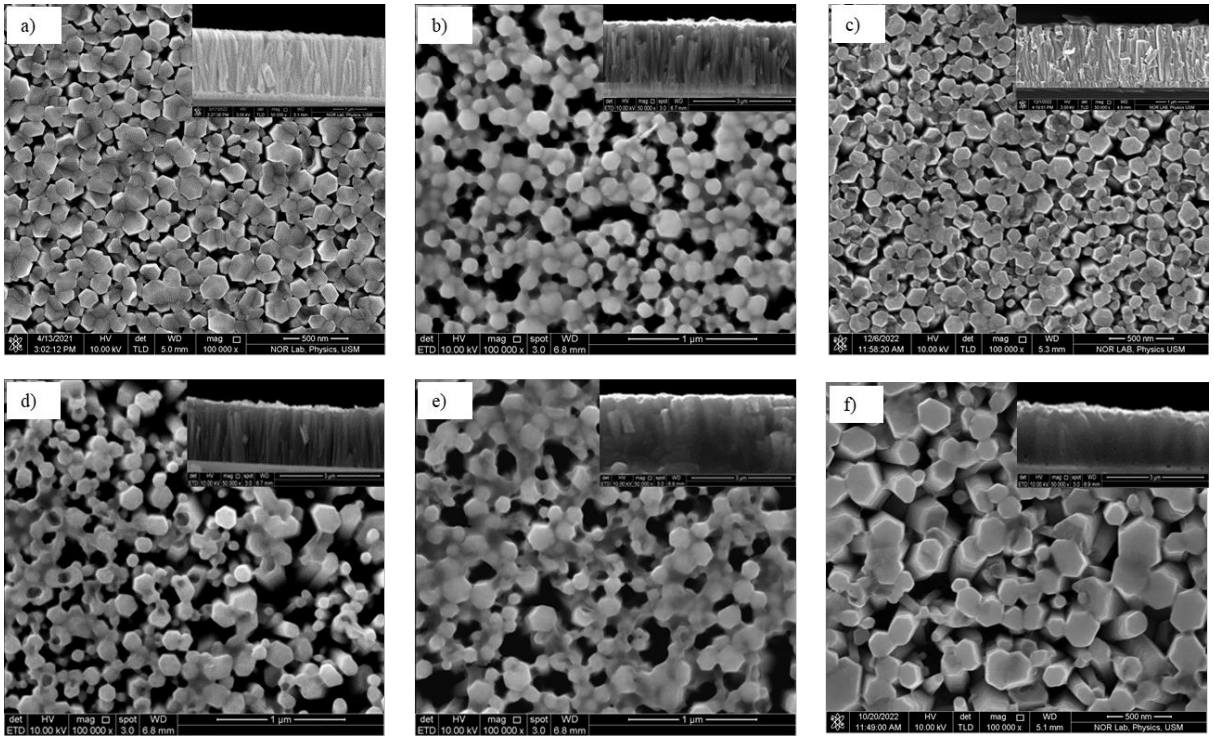

Figure 1: Top view and cross-sectional view (inset) of FESEM images of ZnO nanorods with different times of dipping in aluminum nitrate nonahydrate solution of a) 0 s, b) 20 s, c) 30 s, d) 40 s, e) 60 s, and f) 80 s.

EDX analysis was used to identify the atomic percentage (%) for each element in the samples as summarized in Table 1. The EDX result shows that as the dipping time increases, the atomic percentage (%) of aluminum (Al) rises from 0.81 % to 3.81 %. On the other hand, the zinc (Zn) atomic percentage dropped from 59.65 % to 48.73 % whereas the oxygen (O) atomic percentage increased from 40.35 % to 44.73 %.

Table 1: EDX results of the atomic percentage of elements according to dipping time.

Time of dipping (s)	**Atomic percentage (%)**		
	Zn	**O**	**Al**
0	59.65	40.35	-
20	51.96	47.23	0.81
30	54.04	44.58	1.06
40	51.61	43.70	1.19
60	47.51	48.91	3.57
80	48.73	44.73	3.81

To observe the distribution of the elements, EDX mapping was done for the sample dipped for 40 s as shown in Figure 2. The green colour of the image corresponds to the L-line spectra of the Zn element. Meanwhile, the red and yellow colour images are distinctly acquired at the K-line spectra O and Al elements, respectively. It has been noticed that Zn and O have higher atomic percentages (%) than Al, which may be related to Al's short period of dipping. In

addition, it is observed that the samples prepared are composed only of Zn, O and Al as no other elements were detected.

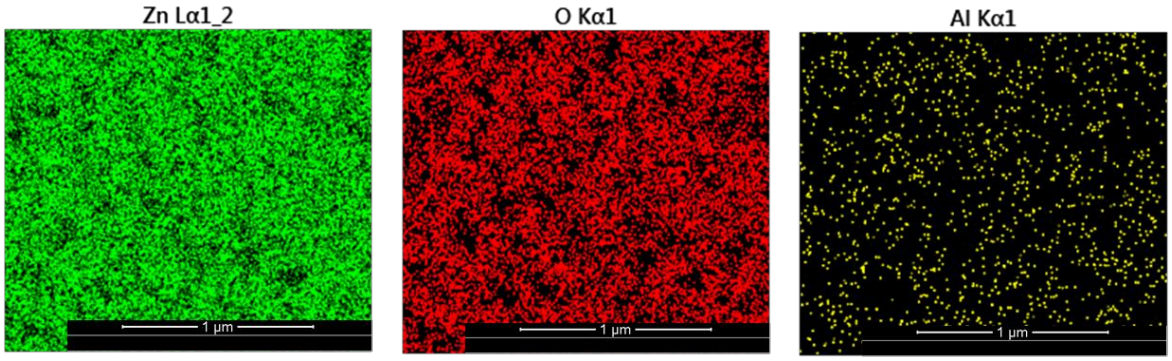

Figure 2: EDX mapping for sample dipped for 40 s. The distribution of the two dominant elements, Zn and O, is consistent with the distribution of nanorods.

Figure 3 shows the XRD pattern for all samples with peaks corresponding to the diffraction planes of (002) and (004). Both peaks were matched with the hexagonal wurtzite structure of ZnO (JCPDS data card number 80-0075). The dominant XRD spectra peak was (002) and the minor peak was (004) due to the preferred orientation along the c-axis. No significant Al peak was observed in the XRD pattern most likely because the Al dopant atoms do not occupy the zinc lattice sites and tend to occupy interstitial sites [34]. In addition, a 0.10° shift to a greater angle was observed in the (002) XRD peak. This is evidence that the crystallite size decreased [35] when doping is introduced and hence shows additional evidence of doping [22], [34].

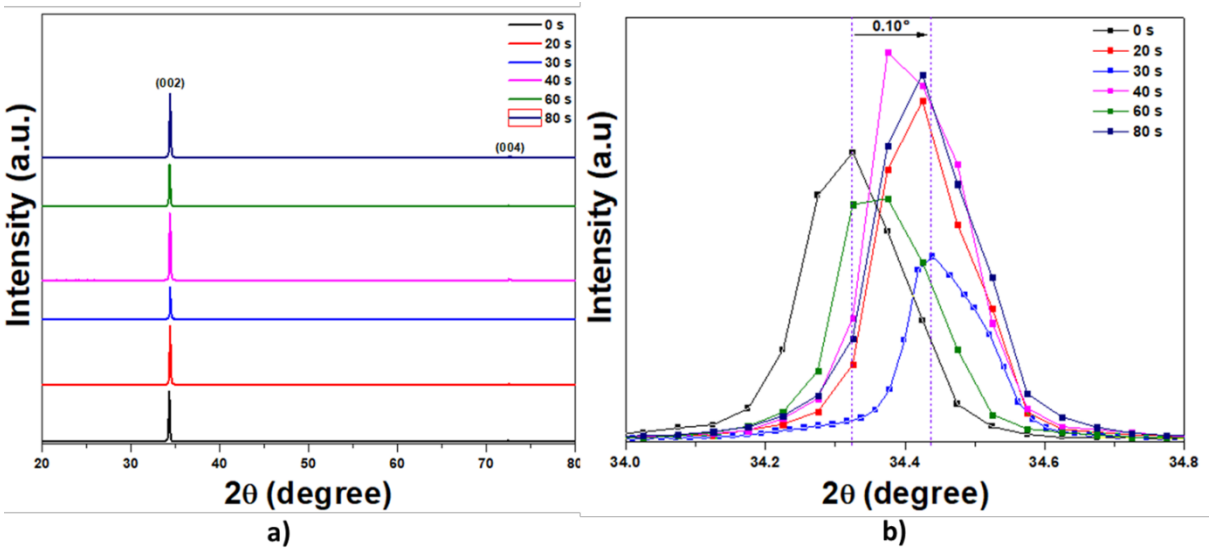

Figure 3: a) The XRD patterns of ZnO nanorods after doping procedure. b) Shift in the (002) diffraction peak due to different doping duration as evidence of doping.

The room temperature PL spectra of ZnO at the different duration of doping is shown in Figure 4. Only near-band edge (NBE) peaks which are related to exciton recombination [36] appeared with narrow peaks centred at 377 nm, 379 nm and 381 nm for different duration of doping. The NBE peaks showed a slight shift of about 4 nm when dipped with different duration of doping.

This is likely to be due to the Burstein-Moss (BM) effect [37], [38]. Note that, pulse excitation (high-intensity excitation) was employed to measure the PL emission, which caused the UV component and the visible component to partially overlap [39]. As a result, only NBE and not deep-level emission (DLE) was observed.

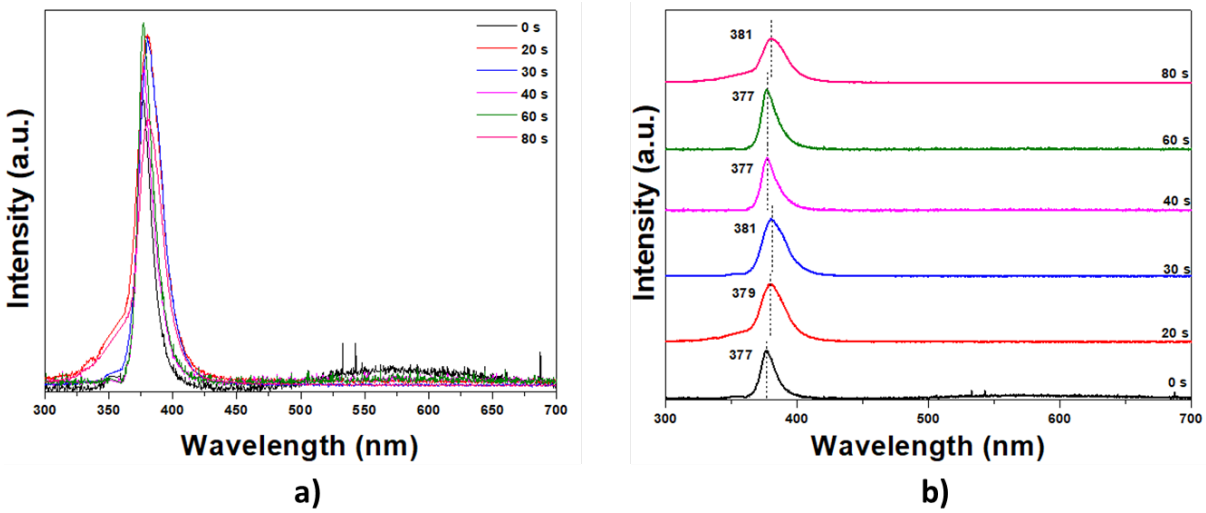

Figure 4: a) PL spectra of samples undergo different dipping duration. b) Zoom in PL spectra of all samples.

Figure 5 a)-e) show random lasing emission observed paired with the pump energy density against the integrated intensity and spectral width measured by the full-width half maximum (FWHM) of the lasing peak from samples that undergo different dip durations of 20 s, 30 s, 40 s, 60 s, and 80 s, respectively. For the 0 s sample, it did not reveal any lasing emission suggesting that doping was required for lasing to occur. All other samples showed random lasing emissions. Different dip duration contributes to different modes formed inside the structure. To generate a particular lasing mode is challenging because light follows a random path in the random media. These modes tend to shift randomly because the random paths taken by subsequent pulses within the medium would be different. Therefore, lasing modes coexist and compete for the available gain so that no specific frequency can dominate, and the random laser can have different spectral features each time it is excited [40]. The threshold values and spectral width for samples undergo doping at 20 s, 30 s, 40 s, 60 s and 80 s were tabulated in Table 2. The lowest threshold energy density 12.48 mJ/cm^2 corresponds to 40 s time of doping (about 1.2 % of Al detected) with a spectral width of 2.12 nm. If Al atoms replace Zn atoms, both scattering and transport mean free path increases [41]–[43]. This then lowers the threshold energy density. Sample doped for 40 s shows the lowest threshold value, implying Al replaced Zn sites and improved the crystallinity. This is evidently shown in the XRD spectrum (Figure 3). Increasing the dip time increased the % of Al in the sample however this does not contribute to improving the lasing emission. In our previous work, lowest threshold was also observed at around this value of Al when doped during growth (in-situ) however it was not possible to investigate beyond 1.7 % as this was the limit in the doping procedure. This current work confirms that doping between 1 and 2 % is ideal for best random lasing as samples above these values showed higher thresholds. It is possible that scattering may be affected with increasing doping. Similarly, grain boundaries have been shown to affect random lasing emission [44] as

such lasing from polycrystalline ZnO nanorods prepared by the same method (i.e. CBD) has also shown to increase threshold [45].

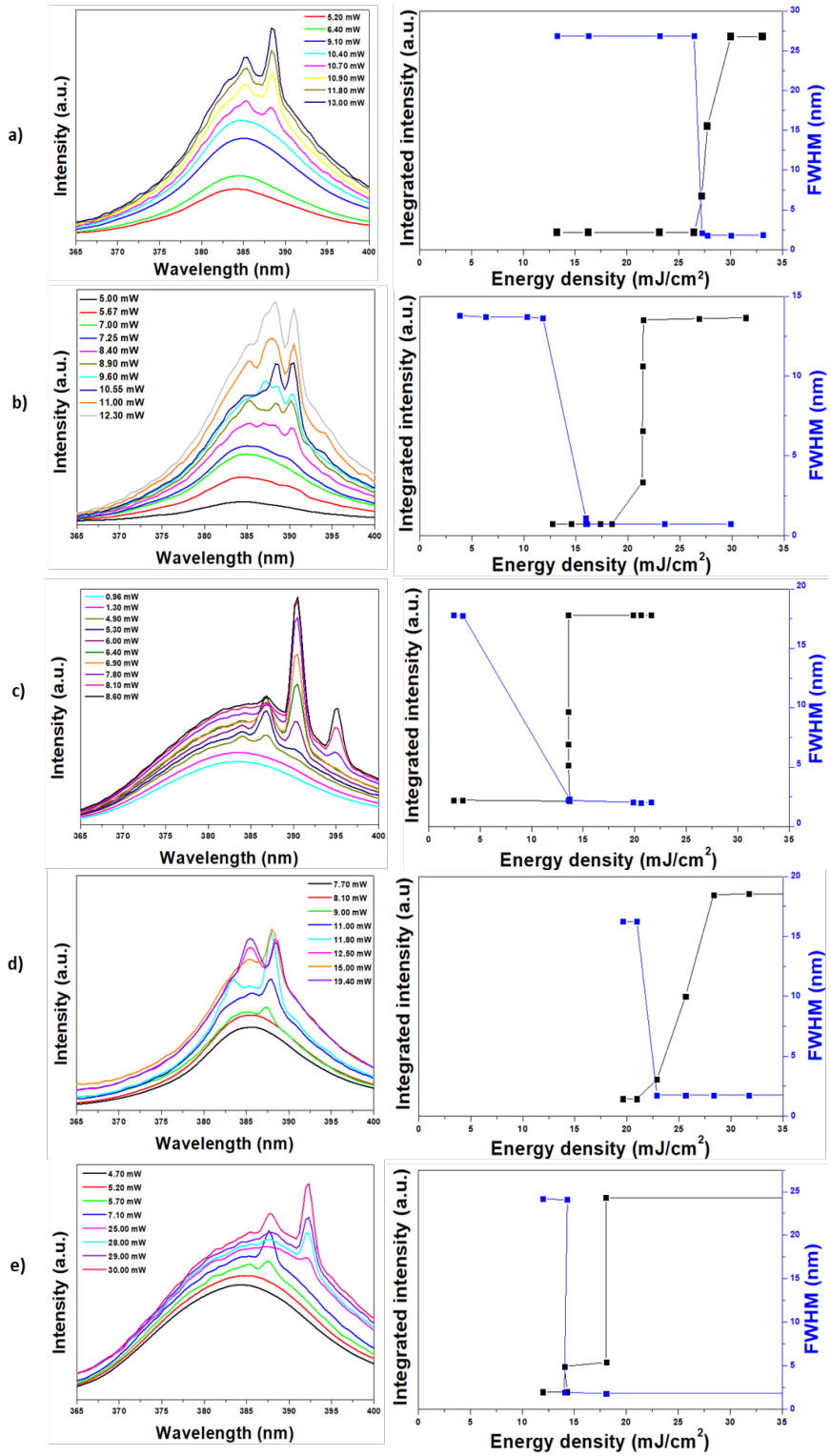

Figure 5: Random lasing measurement paired with the energy density against spectral width measured by the FWHM of lasing peak from samples that undergo different dipping durations of a) 20 s, b) 30 s, c) 40 s, d) 60 s and e) 80 s.

Table 2: Summary of threshold energy density and spectral linewidth based on FWHM for samples with different dip duration.

Time of doping (s)	Threshold energy density (mJ/cm^2)	FWHM (nm)
20	27.25	1.81
30	21.39	0.73
40	12.48	2.12
60	22.92	1.45
80	14.51	1.81

4. CONCLUSION

Ex-situ Al doping in ZnO nanorods was effectively carried out at different doping durations of 0 s, 20 s, 30 s, 40 s, 60 s, and 80 s, respectively. It revealed that the ZnO nanorod structure remained even though the nanorod's height was reduced. In addition, it was observed that the threshold value and spectral width are affected by the Al %, and the random laser cannot occur without doping. This is additional evidence that doping enhances random lasing and lowers the random laser threshold as well. The sample that was doped with Al in aluminum nitrate nonahydrate solution for 40 s resulted in a 1.19 % of Al, a threshold value of 12.48 mJ/cm^2 and a spectral width of 2.12 nm.

ACKNOWLEDGEMENT

This work was supported by Kementerian Pendidikan Malaysia through Fundamental Research Grant Scheme (FRGS) under account number: FRGS/1/2018/STG02/USM/02/6.

CONFLICT OF INTEREST

All authors declare NO conflict of interest.

DATA ACCESS STATEMENT

Access to the research data supporting this publication is available upon request to the corresponding author.

REFERENCES:

[1] R. v Ambartsumyan, N. G. Basov, and P. G. Kryukov, 'A Laser with a Nonresonant Feedback.pdf', *Soviet Physics Jetp*, vol. 24, no. 3, pp. 442–446, 1967.

[2] S. v. Letokhov, 'Generation of light by a scattering medium with negative resonance', *Soviet physics jetps*, vol. 26, no. 4, pp. 835–840, 1968.

[3] N. M. Lawandy, R. M. Balachandran, A. S. L. Gomes, and E. Sauvain, 'Laser action in strongly scattering media', *Nature*, vol. 368, no. 6470, pp. 436–438, 1994, doi: 10.1038/368436a0.

[4] N. Mogharari and B. Sajad, 'Random Laser Emission Spectra of the Normal and Cancerous Thyroid Tissues', *Iran J Sci Technol Trans A Sci*, vol. 43, no. 4, pp. 2055–2060, 2019, doi: 10.1007/s40995-019-00691-8.

[5] F. Lahoz *et al.*, 'Random lasing in brain tissues', *Org Electron*, vol. 75, no. July, p. 105389, 2019, doi: 10.1016/j.orgel.2019.105389.

[6] M. Gaio, S. Caixeiro, B. Marelli, F. G. Omenetto, and R. Sapienza, 'Gain-Based Mechanism for pH Sensing Based on Random Lasing', *Phys Rev Appl*, vol. 7, no. 3, pp. 1–6, 2017, doi: 10.1103/PhysRevApplied.7.034005.

[7] A. L. Moura, P. I. R. Pincheira, L. J. Q. Maia, A. S. L. Gomes, and C. B. de Araújo, 'Two-color random laser based on a Nd3+ doped crystalline powder', *J Lumin*, vol. 181, pp. 44–48, 2017, doi: 10.1016/j.jlumin.2016.09.002.

[8] F. Lahoz *et al.*, 'Random laser in biological tissues impregnated with a fluorescent anticancer drug', *Laser Phys Lett*, vol. 12, no. 4, 2015, doi: 10.1088/1612-2011/12/4/045805.

[9] W. Z. Wan Ismail, G. Liu, K. Zhang, E. M. Goldys, and J. M. Dawes, 'Dopamine sensing and measurement using threshold and spectral measurements in random lasers', *Opt Express*, vol. 24, no. 2, p. A85, 2016, doi: 10.1364/oe.24.000a85.

[10] R. C. Polson, Z. V. Vardeny, R. C. Polson, and Z. V. Vardeny, 'Random lasing in human tissues', vol. 1289, pp. 5–8, 2004, doi: 10.1063/1.1782259.

[11] D. Zhang, Y. Wang, and D. Ma, 'Zno nanorods as scatterers for random lasing emission from dye doped polymer films', *J Nanosci Nanotechnol*, vol. 9, no. 5, pp. 3166–3170, 2009, doi: 10.1166/jnn.2009.024.

[12] W Maryam, H. H. Tan, C. Jagadish, J. M. Dawes, B. Zhao, and WZ Wan Ismail, 'A hybrid random laser using dye with self-organized GaN nanorods', *Semicond Sci Technol*, vol. 37, no. 2, 2022, doi: 10.1088/1361-6641/ac3b3a.

[13] W. Z. W. Ismail, W. M. W. A. Kamil, and J. M. Dawes, 'Enhancement of Random Laser Properties on Solid Polymer Films by Increasing Scattering Effect', *Journal of Russian Laser Research*, vol. 40, no. 4, pp. 364–369, 2019, doi: 10.1007/s10946-019-09812-5.

[14] H. Fujiwara, T. Suzuki, R. Niyuki, and K. Sasaki, 'ZnO nanorod array random lasers fabricated by a laser-induced hydrothermal synthesis', *Optics InfoBase Conference Papers*, 2016, doi: 10.1364/ACOFT.2016.JT4A.9.

[15] Q. Song, L. Liu, S. Xiao, X. Zhou, W. Wang, and L. Xu, 'Unidirectional High Intensity Narrow-Linewidth Lasing from a Planar Random Microcavity Laser', vol. 033902, no. January, pp. 1–4, 2006, doi: 10.1103/PhysRevLett.96.033902.

[16] H. Y. Yang *et al.*, 'Ultraviolet coherent random lasing in randomly assembled SnO2 nanowires', *Applied Physics Letter*, vol. 94, no. 241121, pp. 241121–241121, 2009, doi: 10.1063/1.3157842.

[17] N. Fadzliana, S. A. M. Samsuri, S. Y. Chan, H. C. Hsu, and W. Maryam, 'Influence of Al doping on random lasing in ZnO nanorods', *Opt Laser Technol*, vol. 124, no. November 2019, pp. 1–5, 2020, doi: 10.1016/j.optlastec.2019.106004.

[18] A. T. Ali *et al.*, 'Random laser behavior in Gold-doped Zinc Oxide nanorods structures', in *Journal of Physics: Conference Series*, Nov. 2021, vol. 2075, no. 1. doi: 10.1088/1742-6596/2075/1/012015.

[19] A. T. Ali *et al.*, 'SiO2 Capped-ZnO nanorods for enhanced random laser emission', *Opt Laser Technol*, vol. 147, Mar. 2022, doi: 10.1016/j.optlastec.2021.107633.

[20] P. Zhang, R. Y. Hong, Q. Chen, W. G. Feng, and D. Badami, 'Aluminum-doped zinc oxide powders: Synthesis, properties and application', *Journal of Materials Science: Materials in Electronics*, vol. 25, no. 2, pp. 678–692, 2014, doi: 10.1007/s10854-013-1630-3.

[21] A. Alkahlout, 'A Comparative Study of Spin Coated Transparent Conducting Thin Films of Gallium and Aluminum Doped ZnO Nanoparticles', *Physics Research International*, vol. 2015, 2015, doi: 10.1155/2015/238123.

[22] M. J. Akhtar, H. A. Alhadlaq, A. Alshamsan, M. A. Majeed Khan, and M. Ahamed, 'Aluminum doping tunes band gap energy level as well as oxidative stress-mediated cytotoxicity of ZnO nanoparticles in MCF-7 cells', *Sci Rep*, vol. 5, no. August, pp. 1–16, 2015, doi: 10.1038/srep13876.

[23] S. J. Young and Y. H. Liu, 'High Response of Ultraviolet Photodetector Based on Al-Doped ZnO Nanosheet Structures', *IEEE Journal of Selected Topics in Quantum Electronics*, vol. 23, no. 5, Sep. 2017, doi: 10.1109/JSTQE.2017.2684540.

[24] S.-J. Young, Y.-H. Liu, and L.-T. Lai, 'Fabrication and Characterization of Aluminum-Doped ZnO Nanosheets for Field Emitter Application', *ECS Journal of Solid State Science and Technology*, vol. 6, no. 5, pp. P243–P246, 2017, doi: 10.1149/2.0121705jss.

[25] Y. H. Liu, S. J. Chang, L. T. Lai, Y. P. Tu, and S. J. Young, 'Aluminum-doped zinc oxide nanorods and methyl alcohol gas sensor application', *Microsystem Technologies*, vol. 28, no. 1, pp. 377–382, Jan. 2022, doi: 10.1007/s00542-020-04856-z.

[26] V. Musat, B. Teixeira, E. Fortunato, R. C. C. Monteiro, and P. Vilarinho, 'Al-doped ZnO thin films by sol-gel method', *Surf Coat Technol*, vol. 180–181, pp. 659–662, Mar. 2004, doi: 10.1016/j.surfcoat.2003.10.112.

[27] M. H. Mamat, M. Z. Sahdan, Z. Khusaimi, A. Z. Ahmed, S. Abdullah, and M. Rusop, 'Influence of doping concentrations on the aluminum doped zinc oxide thin films properties for ultraviolet photoconductive sensor applications', *Opt Mater (Amst)*, vol. 32, no. 6, pp. 696–699, 2010, doi: 10.1016/j.optmat.2009.12.005.

[28] D. H. Kim, J. H. Park, T. il Lee, and J. M. Myoung, 'Superhydrophobic Al-doped ZnO nanorods-based electrically conductive and self-cleanable antireflecting window layer for thin film solar cell', *Solar Energy Materials and Solar Cells*, vol. 150, pp. 65–70, Jun. 2016, doi: 10.1016/j.solmat.2016.01.041.

[29] A. T. Ali *et al.*, 'UV random laser in aluminum-doped ZnO nanorods', *Journal of the Optical Society of America B*, vol. 38, no. 9, p. C69, 2021, doi: 10.1364/josab.427132.

[30] M. Advand *et al.*, 'Array of vertically aligned Al-doped ZnO nanorods: Fabrication process and field emission performance', *Thin Solid Films*, vol. 656, pp. 6–13, Jun. 2018, doi: 10.1016/j.tsf.2018.04.008.

[31] S. Edinger *et al.*, 'Comparison of chemical bath-deposited ZnO films doped with Al, Ga and In', *J Mater Sci*, vol. 52, no. 16, pp. 9410–9423, Aug. 2017, doi: 10.1007/s10853-017-1104-8.

[32] I. Volintiru, M. Creatore, and M. C. M. van de Sanden, 'In situ spectroscopic ellipsometry growth studies on the Al-doped ZnO films deposited by remote plasma-enhanced

metalorganic chemical vapor deposition', *J Appl Phys*, vol. 103, no. 3, 2008, doi: 10.1063/1.2837109.

[33] G. Amin, M. H. Asif, A. Zainelabdin, S. Zaman, O. Nur, and M. Willander, 'Influence of pH, precursor concentration, growth time, and temperature on the morphology of ZnO nanostructures grown by the hydrothermal method', *J Nanomater*, vol. 2011, 2011, doi: 10.1155/2011/269692.

[34] A. Samavati *et al.*, 'Structural, optical and electrical evolution of Al and Ga co-doped ZnO/SiO2/glass thin film: Role of laser power density', *RSC Adv*, vol. 7, no. 57, pp. 35858–35868, 2017, doi: 10.1039/c7ra04963c.

[35] K. Mahmood, S. bin Park, and H. J. Sung, 'Enhanced photoluminescence, Raman spectra and field-emission behavior of indium-doped ZnO nanostructures', *J Mater Chem C Mater*, vol. 1, no. 18, pp. 3138–3149, May 2013, doi: 10.1039/c3tc00082f.

[36] B. Efafi, H. Mazandarani, M. H. M. Ara, and B. Ghafary, 'Improvement in photoluminescence behavior of well-aligned ZnO nanorods by optimization of thermodynamic parameters', *Physica B Condens Matter*, vol. 579, Feb. 2020, doi: 10.1016/j.physb.2019.411915.

[37] A. Henni, A. Merrouche, L. Telli, and A. Karar, 'Studies on the structural, morphological, optical and electrical properties of Al-doped ZnO nanorods prepared by electrochemical deposition', *Journal of Electroanalytical Chemistry*, vol. 763, pp. 149–154, Feb. 2016, doi: 10.1016/j.jelechem.2015.12.037.

[38] M. Parvathy Venu, B. Shrisha, K. M. Balakrishna, and K. G. Naik, 'Deposition of undoped and Al doped ZnO thin films using RF magnetron sputtering and study of their structural, optical and electrical properties', in *AIP Conference Proceedings*, May 2017, vol. 1832. doi: 10.1063/1.4980501.

[39] A. P. Tarasov, A. E. Muslimov, and V. M. Kanevsky, 'Stimulated Emission in Vertically Aligned Hexagonal ZnO Microcrystals Synthesized by Magnetron Sputtering Method', *Photonics*, vol. 9, no. 11, p. 871, Nov. 2022, doi: 10.3390/photonics9110871.

[40] J. Bingi, A. R. Warrier, C. Vijayan, J. Bingi, A. R. Warrier, and C. Vijayan, 'Raman mode random lasing in ZnS-β-carotene random gain media', vol. 221105, pp. 1–4, 2013, doi: 10.1063/1.4807668.

[41] K. Totsuka, G. van Soest, T. Ito, A. Lagendijk, and M. Tomita, 'Amplification and diffusion of spontaneous emission in strongly scattering medium', *J Appl Phys*, vol. 87, no. 11, pp. 7623–7628, Jun. 2000, doi: 10.1063/1.373432.

[42] D. J. Durian, 'Influence of boundary reflection and refraction on diffusive photon transport', *Phys Rev E*, vol. 50, no. 2, pp. 857–866, 1994, doi: 10.1103/PhysRevE.50.857.

[43] M. Bahoura and M. A. Noginov, 'Determination of the transport mean free path in a solid-state random laser', *Pol J Environ Stud*, vol. 20, no. 11, pp. 2389–2394, 2005.

[44] M. N. Nordin, M. M. Halim, M. R. Hashim, M. K. Shakfa, and W. Maryam, 'Influence of annealing time on random lasing from ZnO nanorods', *Results Phys*, vol. 16, no. October 2019, p. 102955, 2020, doi: 10.1016/j.rinp.2020.102955.

[45] N. I. M. Tazri, O. L. Muskens, M. K. Shakfa, and W. Maryam, 'Polycrystalline ZnO nanorods for lasing applications', *J Appl Phys*, vol. 125, no. 12, pp. 0–5, 2019**.**